展　望・解　説

Radiation Chemistry of High Temperature and Supercritical Water

Japan Atomic Energy Agency
The University of Tokyo
Mingzhang Lin*
Yosuke Katsumura, Yusa Muroya

The progresses of the studies on water radiolysis at elevated temperatures and supercritical water are reviewed, with the emphasis on the temperature and density effects on the radiolytic yields of water decomposition products, the reaction rate constants and the spectral properties of hydrated electron.

Keywords: water radiolysis, temperature, supercritical water, density effect, picosecond

1 Introduction

The fluids under supercritical conditions exhibit physico-chemical properties drastically different than those usually observed in the liquids or gas phase. The drastic changes of the thermodynamic parameters of the fluid (density, viscosity, thermal conductance, dielectric constant) also affect the reactivity due to the variation of the diffusion constants, the solvent reorganization, and the possible alteration of the ionic-covalent character of the chemical bonds. It has also been demonstrated that, for supercritical water (t_c = 374 °C, P_c = 22.1 MPa, as shown in Figure 1), the hydrogen networking is broken and the water structure possesses the feature of clusters. Accordingly, supercritical fluids offer a range of unusual chemical possibilities such as in environmentally benign separation and destruction of hazardous waste, as well as for new materials synthesis.[1–4)]

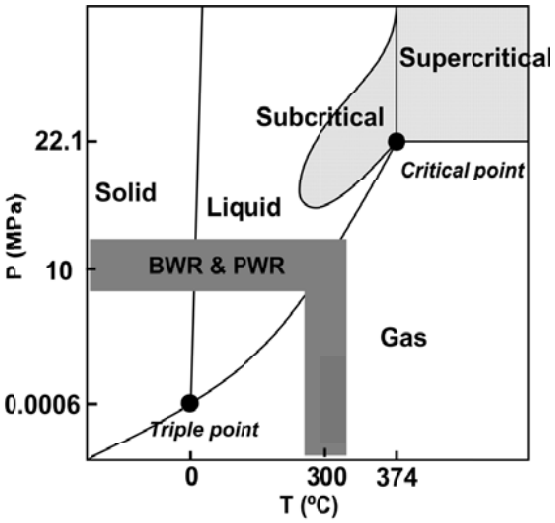

Fig. 1 Schematic representation of the phase diagram of water (H_2O). BWRs or PWRs are operated at constant temperature (280 °C–325 °C) and pressure (15 MPa–20 MPa).

If the studies on water radiolysis at elevated temperatures were motivated by the development of light water reactors, the investigation on the radiolysis of supercritical water should be stimulated by one of the next generation (GenIV) nuclear reactors - supercritical water-cooled reactor (SCWR).[5,6)] This new concept reactor has advantages of higher thermal conversion efficiency, simplicity in structure, and safety, etc. In these reactors, the same as in boiling water reactor (BWR) and pressurized water reactor (PWR), light water or heavy water is used not only as a coolant but also as a moderator. In the reactors, the water is

Radiation Chemistry of High Temperature and Supercritical Water
Mingzhang Lin* (*Japan Atomic Energy Agency*), Yosuke Katsumura and Yusa Muroya (*The University of Tokyo*),
〒319–1195 2–4 Shirane Shirakata Toukai-Mura Naka-Gun Ibaraki Pref., Nuclear Science and Engineering Directorate, Japan Atomic Energy Agency,
TEL & FAX: 029-282-6198, E-mail: lin.mingzhang@jaea.go.jp

exposed to a strong radiation field (≥ 10 kGy/s) composed of γ-rays and 2 MeV fast neutrons, etc. As is well known in the BWR and PWR, two radiolysis products of water, O_2 and H_2O_2, strongly affect the corrosion of structural materials in the reactors. Proper water chemistry controlling, in particular, the injection of H_2 into the coolant to convert O_2 and H_2O_2 into H_2O by radiolytic processes that will effectively reduce the electrochemical corrosion potential (ECP), may represent the key to keep the integrity of the reactors. On the other hand, the basic data about water radiolysis at elevated temperatures might be helpful for the understanding of hydrogen production in case of some accidents, the transportation of nuclear wastes, and the storage or the geological disposal of spent fuel, etc. Computer simulations are usually required to help predict the concentrations of water decomposition products. These simulations require the knowledge of the temperature dependent *G*-values (denoting the experimentally measured radiolytic yields, with unit molecules/100 eV in this context) and rate constants of about 50 reactions. The rate constants and *G*-values of the radiolysis of light and heavy water over the range 0 °C–350 °C have been compiled by Elliot[7,8] and reviewed by Buxton,[9] although most reactions were investigated only up to 200 °C. It is thought that a similar simulation of water radiolysis in SCWR would be required. As is known, BWRs or PWRs are operated at constant temperature (280 °C–325 °C) and pressure (15 MPa–20 MPa). However, according to the current conceptual design of SCWR, the inlet temperature is 280 °C and the outlet temperature is ≥ 500 °C, with a fixed pressure of 25 MPa.[5,6] Thus it is necessary to accumulate the basic data on water radiolysis in a wider temperature range, especially supercritical water which possesses many unusual properties.

We have been engaging in the field of radiation chemistry of supercritical water and alcohols since the end of the 1990s and some of the main results have been introduced in the two books on radiation chemistry published in recent years.[10,11] In this review, we attempt to summarize our studies of radiation chemistry on supercritical water, especially the estimation of *G*-values, the reaction rate constants, the absorption spectral properties of hydrated electron, and the most recent results of the direct measurements of hydrated electron in supercritical water by picosecond pulse radiolysis. Some main results about the spectral properties of solvated electron in various alcohols at elevated temperatures are also introduced.

2 Challenging aspects in experiments

Most of our studies have been carried out using nanosecond pulse radiolysis techniques associated with spectroscopic detection methods. The essential apparatus is the high temperature high pressure (HTHP) flow system. The size, structure and sealing mechanism of the optical windows of the optical cell may vary, but the HTHP system usually consists of a preheater and an optical cell made of high strength and corrosion-resistant alloys such as Hastelloy or SUS316 with sapphire windows. At least one thermocouple should be put into the sample solution inside the cell to monitor the temperature.[12]

The main difficulties for the pulse radiolysis experiments of SCW are listed below:[11]

- Thermal stability of chemical reagents: most of organic compounds are thermally unstable at elevated temperatures, especially in SCW.
- Solubility of inorganic compounds: the dissociation constant is rather small for salts under supercritical conditions; most inorganic compounds are not available.
- Corrosion and damage of the sapphire windows: the sapphire window is easily corroded in SCW, especially under acidic or alkaline conditions, or in the presence of some additives, such as O_2.
- Limitation of detection techniques: dramatically decreasing signal intensity for low density SCW; and many reactions become much faster than at room temperature, requiring a higher time resolution pulse radiolysis system.

3 Radiolytic yield of water decomposition products

As is known, irradiation with electron beam, γ-rays or high-energy charged particles leads to the decomposition of water molecules through excitation and ionization. The radiolysis of water by γ-rays or electron beam is generally expressed as:

$$H_2O \xrightarrow{\gamma, e^-} e^-_{aq}(2.63), H(0.55), OH(2.72), H_2(0.45), H_2O_2(0.68), HO_2(0.026)$$

The values in the parenthesis are of the primary yields in species/100 eV of water decomposition products at room temperature.

3.1 $G(e^-_{aq})$

One suitable scavenging system is the use of 0.5 mM methyl viologen (MV^{2+}) in the presence of *tert*-butanol as OH radical scavenger, under neutral pH condition.[13] Another is the use of 0.5 mM 4,4'-bipyridyl (4,4'-bpy) together with *tert*-butanol in alkaline solution (pH ≥ 11).[14] In both cases, ideally only e^-_{aq} reacts MV^{2+} or 4,4'-bpy to form radical cation $MV^{\bullet+}$ or radical anion 4,4'-$bpy^{\bullet-}$, with fairly strong absorption at 605 nm and ~ 540 nm, respectively. The temperature dependent $G(e^-_{aq})$ from 25 °C to 500 °C at a fixed pressure of 25 MPa is shown in Figure 2. $G(e^-_{aq})$ increases with temperature up to 300 °C, which agrees well with the previous reports. It decreases to a minimum near t_c before jumping to a rather high value at 400 °C, and then it decreases again with increasing temperature up to 500 °C. An independent measurement of $G(e^-_{sol})$ in methanol shows a similar tendency. The big change of $G(e^-_{sol})$ at constant pressure is due to density effects. As displayed in the 3D plots of Figure 3, under supercritical conditions, at a fixed density $G(e^-_{aq})$ decreases with increasing temperature while at a fixed temperature $G(e^-_{aq})$ decreases with increasing water density. Around t_c, the density effect is the most significant, but it becomes less and less as temperature increases.

3.2 $G(e^-_{aq})+G(OH)+G(H)$

Two scavenging systems have been used to evaluate { $G(e^-_{aq})+G(H)+G(OH)$} (denoted as G_{sum} hereafter). One is 0.5 mM MV^{2+} with 0.2 M ethanol, another is 0.5 mM 4,4'-bpy in the presence of 10 mM HCOONa.[13] The solutions are deaerated by Ar gas. Ethanol MV^{2+} and $HCOO^-$ are used to convert $^\bullet$OH radical and $^\bullet$H atom to ethanol radical and $COO^{\bullet-}$, which will subsequently reduce MV^{2+} and 4,4'-bpy to form $MV^{\bullet+}$ and 4,4'-bpyH, the same as those produced by e^-_{aq}, that is, the total yields of $MV^{\bullet+}$ or 4,4'-bpyH should be equal to the total yield G_{sum}. The tendency is very similar to that of $G(e^-_{aq})$. An estimation of the yield of $COO^{\bullet-}$ up to 400 °C by pulse radiolysis of 10 mM sodium formate in N_2O saturated solution well supported these results.[15]

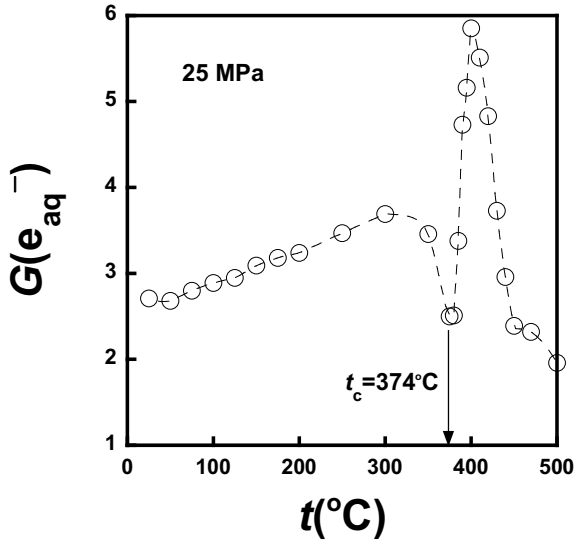

Fig. 2 $G(e^-_{aq})$ as a function of temperature at 25 MPa.

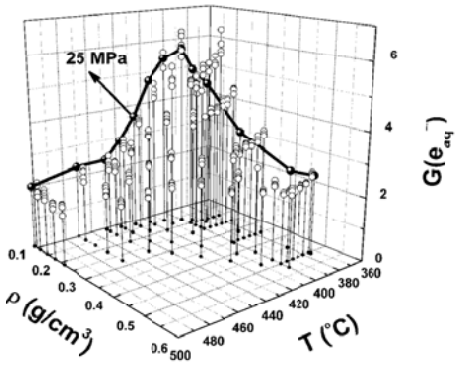

Fig. 3 3D plots of $G(e^-_{aq})$ as a function of temperature and water density. The black curve shows the values at a fixed pressure of 25 MPa.

3.3 $G(OH)$

The estimation of $G(OH)$ has been carried out using an aerated solution of 100 mM $NaHCO_3$ or a deaerated solution of 100 mM $NaHCO_3$ in the presence of 1 mM $NaNO_3$.[11] In these systems, hydrated electrons are scavenged by O_2 or NO_3^- while the reaction between H atoms and HCO_3^- is rather slow. Consequently the yield of $CO_3^{\bullet}$ would be correspond to $G(OH)$. From room temperature to

380 °C, the pressure is 25 MPa while at 400 °C it is 35 MPa because the solubility of $NaHCO_3$ at 400 °C/25 MPa is too small to do the measurements.

4 Reaction rate constants

As mentioned above, for the modeling of water radiolysis in the reactors, the basic data of temperature dependent rate constants are crucial. But the measurements of rate constants at elevated temperatures are rather challenging because of the acceleration of reaction with temperature, especially for the direct kinetics (build-up or decay) method. In addition, this method usually requires a rather low dose to ensure a pseudo-first order decay, but a low dose will certainly result in a small absorbance which already decreases with temperature due to the decrease of water density. Sometimes, competition method is used, but the problem is the lack of suitable competitor with known rate constants at elevated temperatures and SCW.

Despite of the difficulty, extensive studies were devoted to reaction reactivity at temperatures higher than 300 °C or even in SCW in the last decade. The results have demonstrated the unusual behaviors of rate constants at elevated temperatures. Some reactions follow well the linear relationship of Arrhenius equation, while many others exhibit non-Arrhenius behavior. As an example, Figure 4 shows the Arrhenius plots for the reaction of 4,4'-bpy with e^-_{aq}. At 25 MPa, from room temperature to 350 °C, there is a fairly good linear relationship from which an activation energy of 19.6 kJ/mol is calculated.[14] However, it should be pointed out that most reactions do not follow the linear relationship of Arrhenius equation, especially for the temperatures above 200 °C. The inset figure shows the rate constant as a function of water density at 380 °C. Apparently there is a significant density effect on the rate constants. In fact, other studies on the reactions of e^-_{aq} with O_2 and SF_6 in a wider density range exhibit that there is a minimum around 0.45 g/cm^3.[16,17]

5 Absorption spectrum of hydrated electron at elevated temperatures and supercritical water

The optical absorption of hydrated electron e^-_{aq} is characterized by a broad, intense and featureless spectrum which covers most of the visible, tails into the near-infrared, and exhibits a maximum at $\lambda_{max} \sim 718$ nm (or $E_{max} = 1.73$ eV) in H_2O and $\lambda_{max} = 699$ nm (or $E_{max} = 1.77$ eV) in D_2O

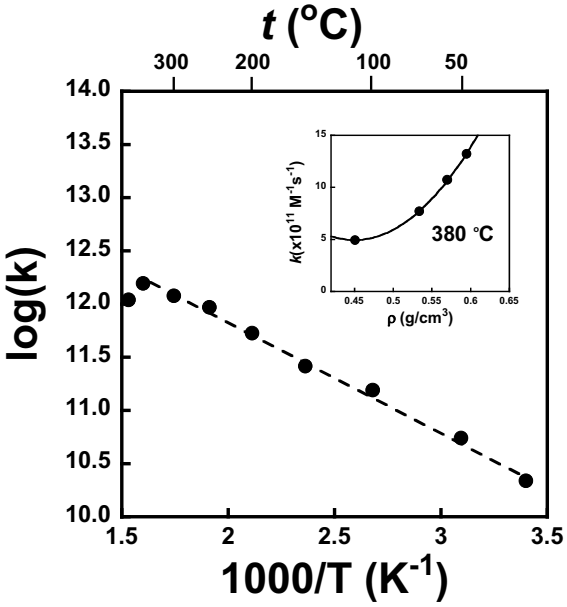

Fig. 4 Arrhenius plots for the reaction of 4,4'-Bpy with hydrated electron. Inset: Rate constant as a function of density at 380 °C. However, many reactions don't obey the linear relationship of Arrhenius equation.

at 25 °C. Temperature effects on e^-_{aq} have been extensively studied using the pulse radiolysis technique and the absorption maximum of e^-_{aq} spectrum is found to shift to longer wavelength with increasing temperature. Typical temperature dependent absorption spectra of e^-_{aq} in D_2O at 25 MPa from room temperature to 390 °C is given in Figure 5. The absorbance largely decreases with temperature because the water density decreases and the decay of e^-_{aq} is accelerated with increasing temperature, as shown in the inset. The fact that e^-_{aq} does exist in SCW and even persists at densities as low as $\sim 8 \times 10^{-3}$ g/cm^3 (limit of the study)[18] indicates that the electron experiences a strong interaction with the neighboring water molecules, implying a dominant role of the short-range molecular structure in the microscopic description of the electron localization and hydration mechanisms.

The absorption spectra of the hydrated electron have been measured by electron pulse radiolysis techniques in supercritical water (D_2O) at different temperatures and densities (or pressures).[19] Over the density range studied ($\sim$ 0.2 g/cm^3–0.65 g/cm^3), the e^-_{aq} absorption maximum

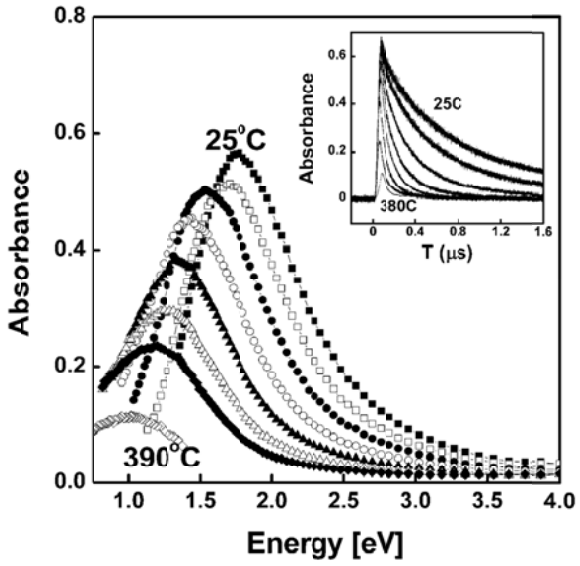

Fig. 5 Absorption spectra of hydrated electron in D_2O under a pressure of 25 MPa at temperatures: 25 °C, 50 °C, 100 °C, 150 °C, 200 °C, 250 °C, 300 °C, and 390 °C. Inset: time profiles at different temperatures of hydrated electron at λ_{max} of each temperature

is found to shift only slightly to the red with decreasing density, in agreement with previous work. Assembling the present data together with those already reported in the literature in sub- and supercritical water shows that $E_{A_{max}}$ varies linearly (in a double logarithmic plot) with density for the various temperatures investigated (namely, 350 °C, 375 °C, 380 °C, 390 °C, and 400 °C) and that the resulting lines are all parallel (within the experimental uncertainties). The temperature dependence of E_{max} in sub- and supercritical D_2O further reveals that, at a fixed pressure (25 MPa), E_{max} decreases monotonically with increasing temperature in passing through the liquid-SCW phase transition at t_c, but exhibits a minimum at a fixed density (0.2 g/cm^3 and 0.65 g/cm^3) as the water passes above t_c into SCW (Figure 6). These behaviors can be understood by means of simple microscopic arguments based on the changes that occur in the water properties and water structure in the sub- and supercritical water regimes. Most importantly, the role of local density and molecular configurational fluctuations (associated with criticality) in providing pre-existing polymeric clusters which act as trapping sites for the excess electron is a pivotal point in the interpretation of the data. By comparison with the $(H_2O)_n^-$ cluster data of Ayotte and Johnson,[21,22] in SCW at 400 °C, the average cluster size is estimated to be ~ 32 water molecules for ρ = 0.65 g/cm^3 and ~ 26 for ρ = 0.2 g/cm^3, respectively. These cluster size values are consistent with reported experimental clustering data on $(H_2O)_n^-$ ions, indicating that interior-bound excess electron states are energetically favored in these sub- and supercritical regions. Electrons residing in such clusters can, alternatively, be viewed as microscopic probes of the local structure of their host environment, and as such, electron solvation experiments present a powerful tool for future studies of the localization of excess electrons in sub- and supercritical water where the dominant role of short-range electron-water interactions is clearly affirmed.

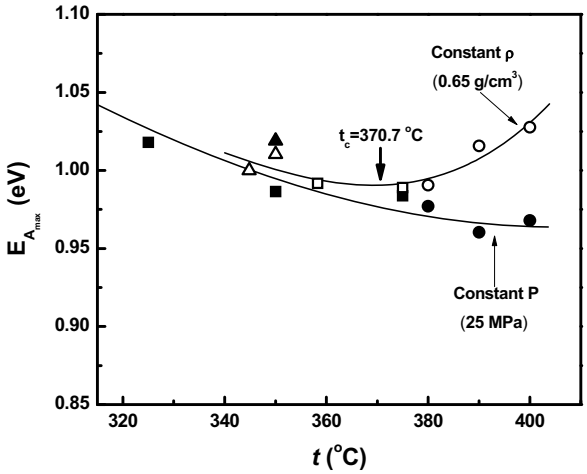

Fig. 6 Absorption maximum of hydrated electron in D_2O (t_c = 307.7 °C, P_c = 21.67 MPa), as a function of temperature at a fixed pressure (25 MPa) and at a fixed density (0.65 g/cm^3). (▲, △) Jortner, et al.[18]; (●, ○) our study[19]; (■, □) Bartels, et al. [20].

Similar studies have been performed on the solvated electron in high temperature and supercritical methanol and ethanol. Similar results, that is, the monotonic decreasing of $E_{A_{max}}$ with temperature and the minimum point corresponding to t_c of the alcohols at a constant density, have been also observed. The sensibility of water containing in methanol on the minimum point of temperature has been demonstrated.[23]

6 Direct observation of the decay kinetics of hydrated electron in supercritical water by picosecond pulse radiolysis[24)]

In order to measure early processes of radiation-induced reactions in high temperature/high pressure water, a new setup was constructed. Usually the radiation induced reactions are very fast. To monitor a reaction from the very beginning of irradiation to the end, it is essential to have a detection technique with high time resolution. Currently, although time resolution of a few picoseconds (1 picosecond = 10^{-12} s) has been achieved by the pulse radiolysis method, it was only available for samples at room temperature. The application of this technique to samples at elevated temperatures or under supercritical conditions resulted in many problems with regard to spectroscopic measurements. The time resolution remained at nanosecond (1 nanosecond = 10^{-9} s). Therefore, in present study a new pulse radiolysis system was developed to overcome those problems.

In order to observe above ultrafast reactions, it is essential to resolve the following two problems:

6.1 Shortening of pulse width and strengthening of the electron beam

First, it is necessary to have a very short radiation pulse. The electron beam used to irradiate the samples must trigger the reaction instantaneously. Besides this, since a larger chemical change due to irradiation will be expected in an easier detection, it is essential to have higher beam intensity. Further, samples at elevated temperatures must be kept in a thick chambered containers, and the electron beam must be able to penetrate this chamber wall. Therefore, a Linac accelerator with a femtosecond laser-driven photocathode, able to generate short pulse width and intense electron beam was used. An electron beam with an energy of ~ 22 MeV and a charge of 2.5 nC–2.8 nC was focused to a diameter of 3 mm. Then it was possible to irradiate the sample inside the vessel with an absorbed dose of 13 Gy/pulse–15 Gy/pulse. In the present work, the intensity of the electron beam was 4–5 times higher than has been used before.

6.2 Measurement of radiation-induced chemical reactions with ultra-high time resolution

To study the radiation induced chemical reactions with the high intensity and short electron pulse discussed above, it is necessary to precisely measure the transient species produced in the sample solutions. Taking advantage of the optical absorption of the transient species, we were able to analyze them by measuring a small change in the light passing through the sample. Using femtosecond laser as the analyzing light, it is possible to have a 'snap-shot' of the sample at a given time after irradiation. So we were able to monitor the reactions dynamically through the difference in the absorptions obtained at the times of irradiation and analysis. Although this method has been used previously for measurements at room temperature, there were problems when applied to the samples at high temperature and high pressure. Because the analyzing light was drastically scattered by the flow of the sample through the optical cell at high temperature and high pressure, it was rather difficult to conduct a precise measurement. In order to resolve this problem, we used two laser pulses with very short time interval (about 11 ns) as reference and analyzing lights, and adjusted the timing of electron beam just between these two laser pulses (i.e. before and after irradiation). Because of the very short interval of these two pulses, we were able to avoid light perturbation due to fluctuation in the sample flow. In addition, a new and unique program for machine controlling, data acquisition and analyzing has been developed. As a result, we have achieved a marked improvement of the precision from ~ 2% to 0.5% .

Accordingly, because of an improvement of 4–5 times in both beam intensity (signal intensity) and measurement precision as compared to previous work, we succeeded in developing a new pulse radiolysis system capable of tracing radiation- induced reactions with picosecond time resolution for high temperature and supercritical water.

As an example, the experimental result using this system is shown in Figure 7, which exhibits the absorption spectra of the hydrated electron recorded at 60 ps after the electron beam pulse. At room temperature, there's a strong absorption band with a maximum at about 700 nm. With increasing temperature, the spectrum shifts to infra-red region and the absorbance decreases. We were able to record

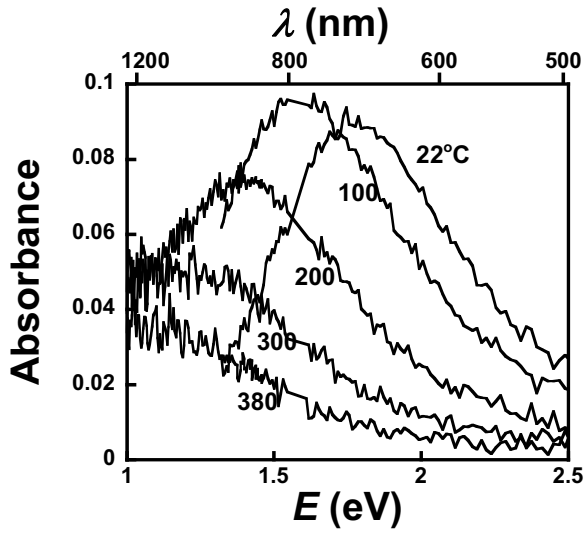

Fig. 7 Absorption spectra of hydrated electron obtained by pulse radiolysis of D_2O from room temperature to supercritical state, recording at 60 ps after the electron beam pulse.

the optical absorption spectrum under supercritical conditions (380 °C/30 MPa) where the absorbance became very small.

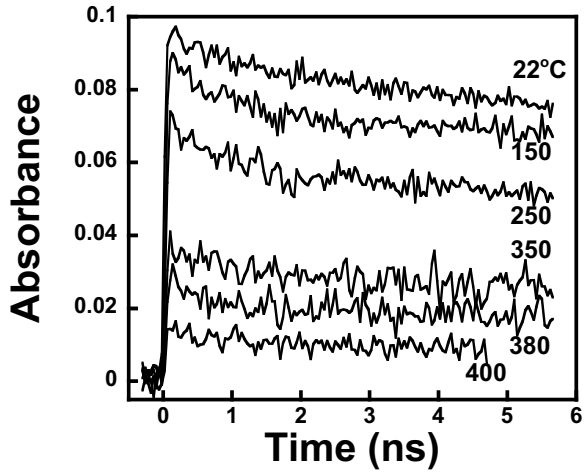

Fig. 8 Temporal behaviors of hydrated electron in D_2O from room temperature to supercritical state.

Meanwhile, we also succeeded in measuring the decay kinetics of hydrated electron from picoseconds to nanoseconds, as shown in Figure 8. At room temperature, it is well known that after formation at very short times (≤ 1 ps) after irradiation, the hydrated electron slowly decays till ~ 100 ns due to spur reactions (complicated reactions between various transient species of water decomposition). For the temporal behaviors at elevated temperatures, there were only a few reports on computer simulations and even for these the temperature was limited to 300 °C. In addition, these reports were different from each other. A model for temperature higher than 300 °C has not been constructed yet. Therefore, the first observation of the decay kinetics of the hydrated electron in the present work is expected to make a significant contribution to the understanding of water radiolysis at elevated temperatures and supercritical conditions.

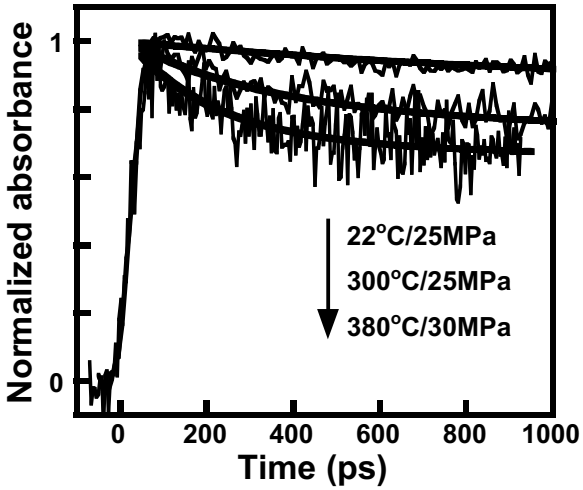

Fig. 9 Temporal behaviors of hydrated electron in D_2O in shorter time region (picoseconds region).

Figure 9 shows a comparison of the temporal behavior of hydrated electron in the picosecond region (≤ 1 ns), from room temperature (22 °C) to high temperature (300 °C) and the supercritical state (380 °C). In each case the signal built up quickly at time zero (immediately after irradiation); however, the decay was clearly different. It is well known that the transient species of water decomposition include $^{\bullet}OH$, $^{\bullet}H$, H^+ H_2 and H_2O_2, in addition to the hydrated electron. At room temperature, very complicated reactions occur among these transients immediately after irradiation to 1 μs. For reactions at elevated temperatures a conventional time resolution of 10 ns was not sufficient to do the measurements. However, with picosecond

pulse radiolysis, we were able to demonstrate that the reactions at elevated temperature (300 °C) became faster than at room temperature and much more drastic under supercritical conditions where 30 % of hydrated electron disappeared within about 600 ps. This implied that the hydrated electron should react with some substances. Possible reactions of the hydrated electron with important water decomposition products e^-_{aq}, OH, H^+ ($e^-_{aq} + {}^\bullet OH \rightarrow OH^-$; $e^-_{aq} + H^+ \rightarrow H^\bullet$; $e^-_{aq} + e^-_{aq} + 2H_2O \rightarrow H_2 + 2OH^-$) can be listed; however, it is likely that the reaction with H^+ will be dominant. The role of this reaction will be elucidated by further experiments.

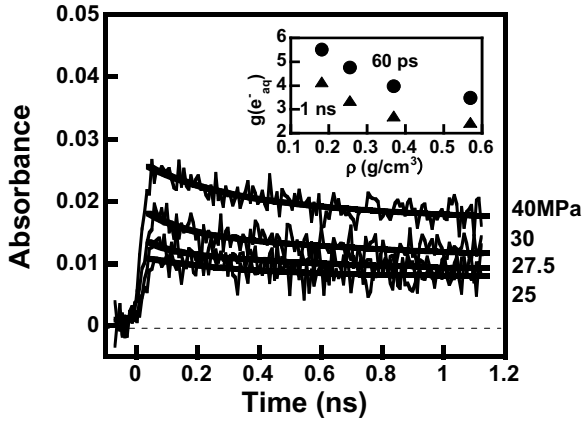

Fig. 10 Time profiles for the decay of hydrated electron at 400 °C under different pressures. Inset: the yields of hydrated electron at 60 ps and 1 ns as a function of water density. The yields were deduced from the time profiles.

Furthermore, the effects of pressure on the temporal behavior of the hydrated electron under supercritical conditions (400 °C) were also investigated. As mentioned above, the water density is greatly dependent on pressure in the supercritical region. For example, in Figure 10, at 400 °C, the water density at 40 MPa is about 3 times higher than at 25 MPa. According to the measurements of the hydrated electron at very different water densities, its yield (*G* value) changed greatly with density, as shown in the inset of Figure 10. The density dependence of the yield of e^-_{aq} at 400 °C agrees well with that obtained by scavenging method. It is noted that not only density but also dielectric constant, ionic product, viscosity, solubility and many other properties change with temperature and pressure. The main factors affecting water radiolysis will be elucidated in the further experiments.

It is worth mentioning that, following the measurements of solvated electron in water and alcohols, the direct observation of hydroxyl radical ($^\bullet OH$) by picosecond pulse radiolysis at room temperature has been successfully carried out.[25] Due to its absorption in deep UV, the non-negligible contribution of the irradiated quartz cell is understood. This sheds some light on the direct measurements of $^\bullet OH$ in the future.

7 Radiolysis of alcohols at elevated temperatures

There are at least two reasons why we are interested in the studies of solvated electrons in high temperature and supercritical alcohols. First, the molecular structure of simple alcohols such as methanol is similar to that of water while their supercritical conditions are much milder than water, for example, the critical temperature (t_c) and pressure (P_c) of methanol are 239.5 °C and 8.1 MPa, but for H_2O, they are 374 °C and 22.1 MPa, respectively. The investigation is expected to be helpful for a better understanding of the radiolysis of water at elevated temperatures and supercritical water. The second reason is due to the variety and intrinsic properties of alcohols. Structurally, alcohols can have different chain length (C number) and OH group number. Their polarity (dielectric constant) and viscosity are quite different from those of water and also strongly correlated with the chemical structure. These will eventually affect the solvation processes of electron.

Figure 11 shows t the transition energy at the absorption maximum plotted as a function of temperature for the solvated electron in some primary alcohols (methanol, ethanol, 1-propanol, 2-propanol, 1-butanol, 1-pentanol, 1-hexanol, and 1-octanol) and four poly-alcohols, ethane-1,2-diol (12ED), propane-1,2-diol (12PD), and propane-1,3-diol (13PD), that we investigated in recent years.[26–32] In general, by increasing the temperature, the decays become faster and most of the solvated electrons disappear within the electron pulse due to the geminate recombination. However, it can be clearly observed that the maximum of the solvated electron absorption band shifts to the longer wavelength with the temperature rise. For the primary alcohols (*n*-alcohols), the temperature coefficient increases with increasing chain length. For the alcohols with same chain length and OH numbers, temperature coefficient is larger for the symmetric alcohols than the asym-

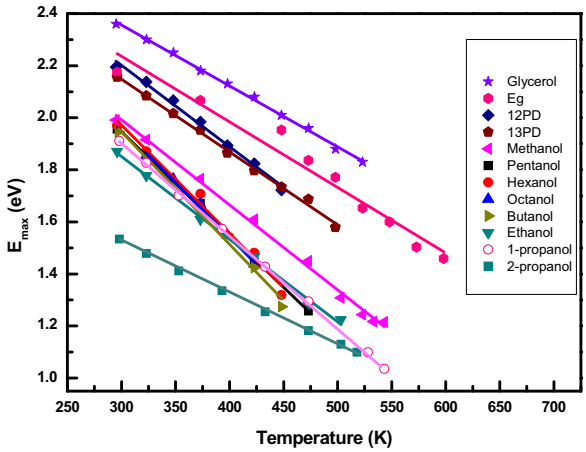

Fig. 11 Transition energy at the absorption maximum as a function of temperature for the solvated electron in various alcohols.

metric ones.

Very interestingly, for the solvated electron in poly-ols, the red-shift of the spectrum with increasing temperature corresponds very well with the spectral shift of electron solvation obtained by femtosecond laser photolysis, that is, higher temperature corresponds to shorter time.[25,26,28,31] For example, in the case of glycerol,[30] the spectra at 125 °C, 100 °C, and 75 °C agree fairly well with those at 100 fs, 3 ps, and 20 ps, respectively. The blue shift of the absorption spectrum of the electron during solvation in poly-ols is continuous and can be described by the temperature dependent absorption spectrum of the ground state solvated electron, suggesting that the blue shift is caused mostly by the thermal relaxation of the solvated electron.

With a combination of scavenging method and direct measurement using picosecond pulse radiolysis, the temporal behaviours of e^-_{sol} in the four poly-ols at room temperature have been studied. The temperature effects on the decay kinetics of solvated electron in methanol from picoseconds to microseconds have been also observed from room temperature to supercritical conditions.

8 Conclusions

Under sub- or supercritical conditions, the radiolytic yields of water decomposition products, the reaction rate constants and the spectral properties of transient species show significant different from those of water at ambient condition or even at elevated temperatures below 300 °C. These properties are not only dependent on temperature but also greatly affected by water density in SCW, or in other words, they exhibit non-linear behaviors or even non-monotonic function with temperature at a fixed pressure. This would strongly suggest a re-consideration of current model of water radiolysis in nuclear reactors, especially for the future SCW reactors. On the other hand, these unusual behaviors are certainly related to the peculiar water properties and water structure of SCW such as dielectric constant, hydrogen bonding network, clustering, and density inhomogeneity, etc. This requires more fundamental studies on temperature effects of the electron solvation processes, the spur reaction processes and other more general chemical interests in these intriguing reaction media. Besides the experimental work, computer simulations are expected to be helpful for a better understanding of the physical nature of these effects. Fortunately, in collaboration with Prof. Jay-Gerin's group, some progresses have been made recently in the evaluation of the time of spur expansion in the low-LET high-temperature water radiolysis,[33] and also the re-examination of the radiolytic yields of water decomposition products by low-LET radiation,[34] using Monte-Carlo simulations, though the highest temperature is still limited to 350 °C.

9 Acknowledgments

We wish to acknowledge the group of Prof. M. Mostafavi at the Universite de Paris-Sud, and that of Prof. J-P. Jay-Gerin, for the collaborated work and valuable discussions. We are thankful to Dr. H. He, Dr. T. Miyazaki, Dr. H. Fu, Dr. Z. Han, Dr. S. Yamashita, and other researchers and students who have contributed to those related studies. We are also grateful to Mr. T. Ueda and Prof. M. Uesaka for their technical assistance in pulse radiolysis experiments and encouragement.

References

1) P. G. Jessop, T. Ikariya, R. Noyori, Nature, 368 (1994) 231.
2) P. E. Savage, S. Gopalan, T. I. Mizan, C. J. Martino, E. E. Brock, Aiche J., 41 (1995) 1723.
3) C. A. Eckert, B. L. Knutson, P. G. Debenedetti, Na-

ture, 383 (1996) 313.
4) N. Akiya, P. E. Savege, Chem. Rev., 102 (2002) 2725.
5) Y. Oka, K. Kataoka, Annual Nucl. Energy, 19 (1992) 243.
6) D. Squarer, T. Schulenberg, Y. Oka, D. Bittermann, N. Aksan, Y. C. Maracz, R. Kyrki-Rajamaeki, A. Souyri, P. Dumaz, Nucl. Eng. Des., 221 (2003) 167.
7) A. J. Elliot, D. M. Bartels, Report AECL No. 153-127160-450-001, Atomic Energy of Canada Limited, Chalk River, Ontario, Canada, 2009.
8) A. J. Elliot, D. C. Ouellette, C. R. Stuart, Report No. AECL-11658, COG-96-390-1, 1996.
9) G. V. Buxton, High temperature water radiolysis, in: C. D. Jonah, B. S. M. Rao (Eds.), Radiation chemistry—Present status and future trends, Elsevier, Tokyo, 2001, pp. 145–162.
10) M. Lin, Y. Muroya, G. Baldacchino, Y. Katsumura, Radiolysis of Supercritical Fluids, in: J. F. Wishart, B. S. M. Rao (Eds.), Recent Trends in Radiation Chemistry, World Scientific Publishing Company, 2010, pp. 255–277.
11) M. Lin, Y. Katsumura, Radiation Chemistry of High Temperature and Supercritical Water and Alcohols, in: Y. Hatano, Y. Katsumura, A. Mozumder (Eds.), Charged Particle and Photon Interactions with Matter: Recent Advances, Applications, and Interfaces, Taylor and Francis, 2010, pp. 401–424.
12) M. Mostafavi, M. Lin, G. Wu, Y. Katsumura, Y. Muroya, J. Phys. Chem. A, 106 (2002) 3123.
13) M. Lin, Y. Katsumura, Y. Muroya, H. He, G. Wu, Z. Han, T. Miyazaki, H. Kudo, J. Phys. Chem. A, 108 (2004) 8287.
14) M. Lin, Y. Katsumura, H. He, Y. Muroya, Z. Han, T. Miyazaki, H. Kudo, J. Phys. Chem. A, 109 (2005) 2847.
15) M. Lin, Y. Katsumura, Y. Muroya, H. He, T. Miyazaki, D. Hiroishi, Radiat. Phys. Chem., 77 (2008) 1208.
16) J. Cline, K. Takahashi, T. W. Marin, C. D. Jonah, D. M. Bartels, J. Phys. Chem. A, 106 (2002) 12260.
17) T. W. Marin, J. A. Cline, K. Takahashi, D. M. Bartels, C. D. Jonah, J. Phys. Chem. A, 106 (2002) 12270.
18) J. Jortner, A. Gaathon, Can. J. Chem., 55 (1977) 1801.
19) J-P. Jay-Gerin, M. Lin, Y. Katsumura, H. He, Y. Muroya, J. Meesungnoen, J. Chem. Phys., 129 (2008) 114511.
20) D. M. Bartels, K. Takahashi, J. A. Cline, T. W. Marin, C. D. Jonah, J. Phys. Chem. A, 109 (2005) 1299.
21) P. Ayotte, M. A. Johnson, J. Chem. Phys., 106 (1997) 811.
22) J. V. Coe, Int. Rev. Phys. Chem., 20 (2001) 33.
23) Y. Yan, M. Lin, Y. Katsumura, Y. Muroya, S. Yamashita, K. Hata, J. Meesungnoen, J-P. Jay-Gerin, Can. J. Chem., 88 (2010) 1026.
24) Y. Muroya, M. Lin, V. de Waele, Y. Hatano, Y. Katsumura, M. Mostafavi, J. Phys. Chem. Lett., 1 (2010) 331.
25) A. K. EL Omar, U. Schmidhammer, P. Jeunesse, J. P. Larbre, M. Lin, Y. Muroya, Y. Katsumura, P. Pernot, M. Mostafavi, J. Phys. Chem. A, 115 (2011) 12212.
26) M. Mostafavi, M. Lin, H. He, Y. Muroya, Y. Katsumura, Chem. Phys. Lett., 384 (2004) 52.
27) I. Lampre, M. Lin, H. He, Z. Han, M. Mostafavi, Y. Katsumura, Chem. Phys. Lett, 402 (2005) 192.
28) Z. Han, Y. Katsumura, M. Lin, H. He, Y. Muroya, Chem. Phys. Lett., 404 (2005) 267.
29) M. Lin, M. Mostafavi, Y. Muroya, Z. Han, I. Lampre, Y. Katsumura, J. Phys. Chem. A, 110 (2006) 11404.
30) M. Lin, M. Mostafavi, Y. Muroya, I. Lampre, Y. Katsumura, Nucl. Sci. Tech., 18 (2007) 2.
31) Z. Han, Y. Katsumura, M. Lin, H. He, Y. Muroya, H. Kudo, Radiat. Phys. Chem., 77 (2008) 409.
32) M. Lin, H. Fu, I. Lampre, V. de Waele, Y. Muroya, Y. Yan, S. Yamashita, Y. Katsumura, M. Mostafavi, J. Phys. Chem. A, 113 (2009) 12193.
33) S. Sanguanmith, Y. Muroya, T. Tippayamontri, J. Meesungnoen, M. Lin, Y. Katsumura, J-P. Jay-Gerin, Phys. Chem. Chem. Phys., 13 (2011) 10690.
34) S. Sanguanmith, Y. Muroya, J. Meesungnoen, M. Lin, Y. Katsumura, L. M. Kohan, D. A. Guzonas, C. R. Stuart, J-P. Jay-Gerin, Chem. Phys. Lett., 508 (2011) 224.

〈著 者 略 歴〉

Mingzhang Lin： 1988 年 中国科学技術大学 卒業. 1991 年 中国科学技術大学 修士修了. 1996 年 Universite de Paris-Sud, 博士修了. 1999 年 中国科学技術大学 副研究員. 2000 年 東京大学 博士研究員. 2007 年 日本原子力研究開発機構 任期付研究員（2008 年から副主任研究員）.

Yosuke Katsumura： 1972 年 東京大学 卒業. 1974 年 東京大学 修士修了. 1976 年 東京大学 助手. 1984 年 東京大学 助教授. 1994 年 東京大学 教授.

Yusa Muroya： 1998 年 東京大学 卒業. 2000 年 東京大学 修士修了. 2001 年 東京大学 助手（2007 年から助教）. 2007 年 博士（工学）東京大学. 2008 年 早稲田大学 客員講師.